Journal of Materials Chemistry A

Accepted Manuscript

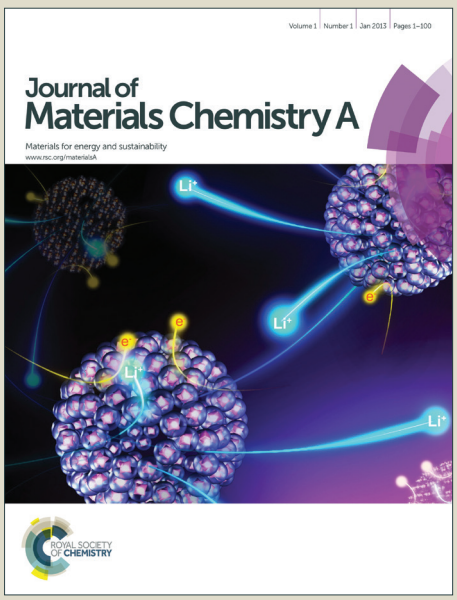

ROYAL SOCIETY OF CHEMISTRY

www.rsc.org/materialsA

Journal Name

RSCPublishing

ARTICLE

Exceeding the Filling Fraction Limit in $CoSb_3$ Skutterudite: Multi-Role Chemistry of Praseodymium Leading to Promising Thermoelectric Performance

Cite this: DOI: 10.1039/xoxxoooooox

Received ooth January 2012,
Accepted ooth January 2012

DOI: 10.1039/xoxxoooooox

www.rsc.org/

J. W. Graff, X. Zeng, A. M. Dehkordi, J. He, and T. M. Tritt*,

To this date and to the best of our knowledge, Praseodymium (Pr), has not been reported for an experimental investigation of its thermoelectric (TE) properties as a potential filler atom in the $CoSb_3$-based skutterudite structure. In addition, reports on skutterudite compounds suggest enhancement in TE properties can occur when the filling fraction limit (FFL) is exceeded resulting in *in situ* secondary phases developing during synthesis. The results reported herein confirm important new concepts due to the multi-role chemistry of the Pr added Co_4Sb_{12} skutterudites (i.e. $Pr_yCo_4Sb_{12}$,), including: 1) Exotic behavior in the Seebeck coefficient, α, as Pr is introduced to the matrix 2) An increase in ZT_{max} (≈ 1.0 at T ≈ 800 K) and the temperature range for ZTmax as Pr is increased and 3) Confirmation of secondary phase(s) aiding in the improvement of TE properties.

Introduction

Despite novel technical merits, thermoelectric (TE) devices are currently used in niche markets where the concern of reliability exceeds performance and cost. Broader applications of TE devices thus hinge upon developing high performance environmentally friendly TE materials, and $CoSb_3$-based skutterudites have proven to be a prime example of such materials. The performance of a TE material is governed by its dimensionless figure of merit, $ZT = (\alpha^2\sigma T)/\kappa$, where α is Seebeck coefficient, σ electrical conductivity, κ thermal conductivity, and T temperature in Kelvin. While there is no known theoretical upper limit for *ZT*, the state-of-the-art TE materials have maximum $ZT \sim 1\text{-}2$ due to adversely inter-related α, σ, and κ where optimizing one quantity often unfavorably affects the others. Typically, it takes a concerted effort to tune multiple control parameters simultaneously in order to ease the inter-dependence of α, σ, and κ for an enhancement in *ZT*. It is rare to observe simultaneous optimization of all three TE properties[1], not to mention attaining a state-of-the-art *ZT* in an extensively studied TE material via only one control parameter.

The work presented herein successfully *optimizes all three TE properties of a Skutterudite resulting in a state-of-the-art ZT via one control parameter: the addition of Praseodymium (Pr).* The approach builds on the multiple chemistry roles of Pr in the $CoSb_3$ skutterudite system, including, (*i*) filling the naturally formed voids in the crystal structure, (*ii*) forming secondary phase nano-inclusions on the grain boundaries, and (*iii*) tuning of the electronic band structure via doping. The interplay between these three roles gives rise to two noteworthy phenomena, (*i*) a 5-fold increase in *ZT* upon Pr addition above the filling fraction limit (FFL) in Co_4Sb_{12}, (i.e. $Pr_yCo_4Sb_{12}$,), and (*ii*) the Pr impurities driving Co_4Sb_{12} from *p*-type to *n*-type in α across the FFL with exotic behavior in α arising at low Pr concentrations.

Specifically, our approach is a paradigm shift from the traditional "filling-rattling" approach to a combined "filling + *in situ* nanostructuring" approach via purposefully exceeding the FFL of Pr in the Co_4Sb_{12} skutterudite. The results shed new light on how to overcome the two inherent restrictions, namely, the FFL and rattling of the filler atoms in the study of TE properties of skutterudites and other cage-like TE materials.

The unit cell of Co_8Sb_{24} skutterudite comprises 32 atoms with a cubic Co framework, with six antimony rings occupying 6 cages (quadrant cubicles), and two empty cages. The two empty cages can be filled with guest elements acting as "rattlers", which are large loosely bound heavy ions that hop or tunnel between the multiple energy minima within the cage.[2-4] The most complete form of the unit cell is written as $\square_2Co_8Sb_{24}$ where the □ represents the voids or cages. We will use the formulization of ½ the unit cell in this description, $Pr_yCo_4Sb_{12}$, for simplicity. Many scopes of study note the decoupling dynamics of the guest atom on the relationship between independent localized "rattling" modes and low lattice thermal conductivities.[5-8] In this vein, single-[9-16], double-[17-22], and multiple-filling[23-27] have been successfully implemented in skutterudites. Specifically, a marked reduction in lattice thermal conductivity via single-filling with *in situ* formed nanocomposites is first reported in Zhao et al.[11] However, this "rattler" approach, by multiple-filling of skutterudites, is reaching a TE performance cap of $ZT \approx 1.6$[23-27]. To the contrary, it has been shown, quite recently by phonon dispersion relation measurements, that the resulting lower

lattice thermal conductivities are more likely a consequence of anharmonicity of vibrations within the lattice, and not specific inelastic resonance effects associated by the energy dissipation of isolated "rattlers".[28-29] However, there still remains on-going debate on the topic.

The FFL is, however, the predicted limit for further reduction of lattice thermal conductivity via the traditional filling-rattling approach, [30] hence alternate approaches involving both electronic and thermal improvement are highly desirable.[31] To this end, we select a scarcely studied filler element Pr and build an approach to answer the question: *what would occur if the theoretical FFL of Pr is exceeded* in the Co_4Sb_{12} skutterudite? i.e. Can we successfully create Pr-rich thermoelectrically beneficial *in situ* nanostructures by filling the skutterudite beyond the theoretical FFL of Pr? In general, the FFL is determined by an element's electronegativity, ionic radius, and valence states. Some studies have shown that exceeding the theoretical FFL in skutterudites can create *in situ* secondary phases that have been identified as possible sources for improvement in their TE properties, i.e., acting as phonon scattering mechanisms and thus reducing thermal conductivity and/or enhancing electrical conduction. [18] Furthermore, despite a typically good agreement between theoretical and experimental values of the FFL, there are notable exceptions. For example, Neodymium (Nd) has an experimental FFL a factor of 3 higher than its theoretical value.[32] Hence it motivates the present study on Pr in Co_4Sb_{12}, (i.e. $Pr_yCo_4Sb_{12}$,), chemically similar to Nd. To the best of our knowledge, this manuscript is the first to report the experimental TE properties of single-filled $Pr_yCo_4Sb_{12}$. Pr-filled single crystal skuttuerdites, such as $PrCoAl_3$, $PrOsSb_3$, $PrRuP_3$, and $PrRuSb_3$ have been studied in detail for their intriguing ground state properties which is important as a basis for understanding their excited state behavior presented herein.[33-38]

This idea of *exceeding the theoretical FFL*, using a single-filler Pr (the only control parameter), is at the core of the manuscript presented by exploring the full potential for enhancement of TE properties, specifically in the previously uninvestigated Pr filled Co_4Sb_{12} systems. Furthermore, this approach can be applied to all previously unstudied skutterudite and clathrate TE materials, either individually or employed in tandem with other experimental approaches.

Experimental

According to Shi *et. al.*, the theoretical FFL of single-filled Pr in the Co_4Sb_{12}-based skutterudite is 7 *at%* [32]. For this reason, samples $Pr_yCo_4Sb_{12}$ ($0 < y < 0.8$) were synthesized and their thermal and electrical properties were characterized. Samples of $Pr_yCo_4Sb_{12}$ ($0 < y < 0.8$) were prepared using a melt-anneal-sintering procedure described elsewhere [27]. The as-sintered samples, using spark plasma sintering SPS (using a Dr. Sinter Lab, SPS-515S), are in the shape of a disc and are within ~ 86% of the theoretical density. Maximum sintering temperatures and pressures were used to create the most homogeneous and densified skutterudite samples[39]. Resulting pellets were examined by high resolution powder X-ray diffractometry (HRXRD) (using a Rigaku Ultima IV) for compositional analysis verifying Co_4Sb_{12} as the primary phase with additional secondary phase Pr_2O_3 only detectable in sample y = 0.4 (see †supplemental material). Energy dispersive X-ray spectroscopy (EDS) mapping indicates that Pr takes on several chemical roles within the skutterudite. Pr fills the void spaces, conglomerates as Pr-rich regions at the edges of the grains, and forms a Pr-containing nano-sized secondary phase along the grain boundaries (in higher Pr concentrated samples). Scanning electron microscopy (SEM) confirms average grain sizes of all samples to be ≈10-20 μm. Electrical and thermal transport properties were measured from approximately 10 K to 650 K. Low temperature (10 K – 300 K) (using a custom designed resistivity and Seebeck measurement system and a custom designed thermal conductivity measurement system)[40-41] and high temperature (300 K – 650 K) (using an Ulvac Riko® ZEM II and Netzch Microflash® 457) measurements were taken on four separate systems and the data is well matched (as observed in **Figure 1(a)**). Heat capacity (C_p) measurements were performed (using a Pegasus® 404 DSC) on select samples from 320 K to 775 K showing no peaks with thermo-chemical stabilization before and after each run; thus, verifying the stability of the secondary phase. All samples follow well with the Dulong Petit limit and heat capacity values are within 95% of one another. Samples were reproduced via the melt-anneal-sintering program confirming homogeneity and accuracy of TE properties.

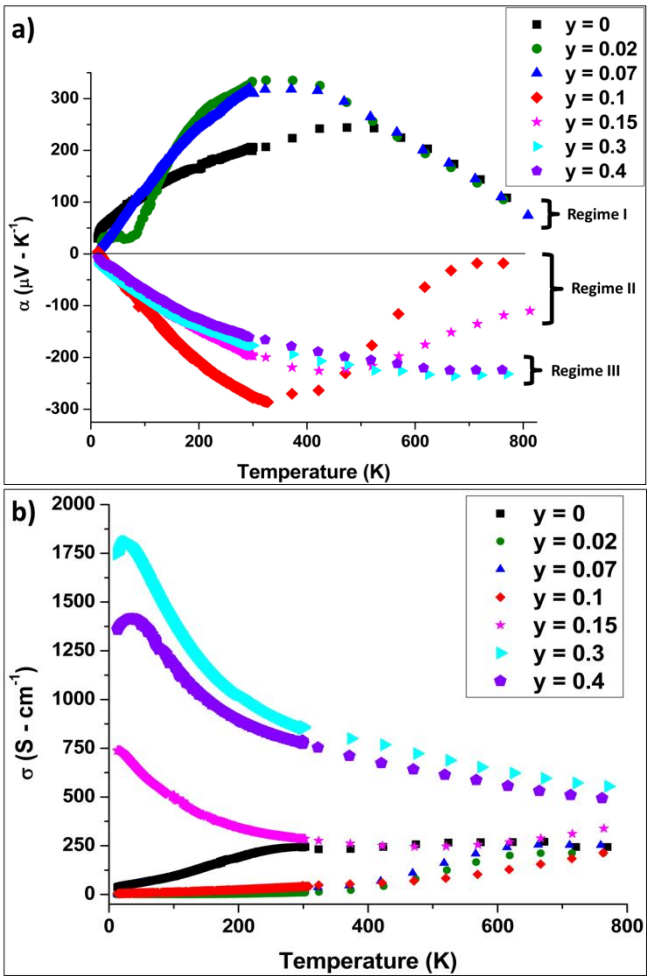

Figure 1. The temperature dependence of the TE properties of $Pr_yCo_4Sb_{12}$ ($0 < y < 0.8$). **a)** Seebeck coefficient (α) emphasizing the transition from *p*-type to *n*-type with 3 regime's divided into low (**I**) mid (**II**) and high (**III**) Pr concentrations, and of **b)** electrical conductivity (σ) with the 3 regimes displaying various temperature behaviors including semiconductor type behavior (**regime I**), semimetal or degenerate semiconductor type behavior (**regime III**), and behaviors in between (**regime II**).

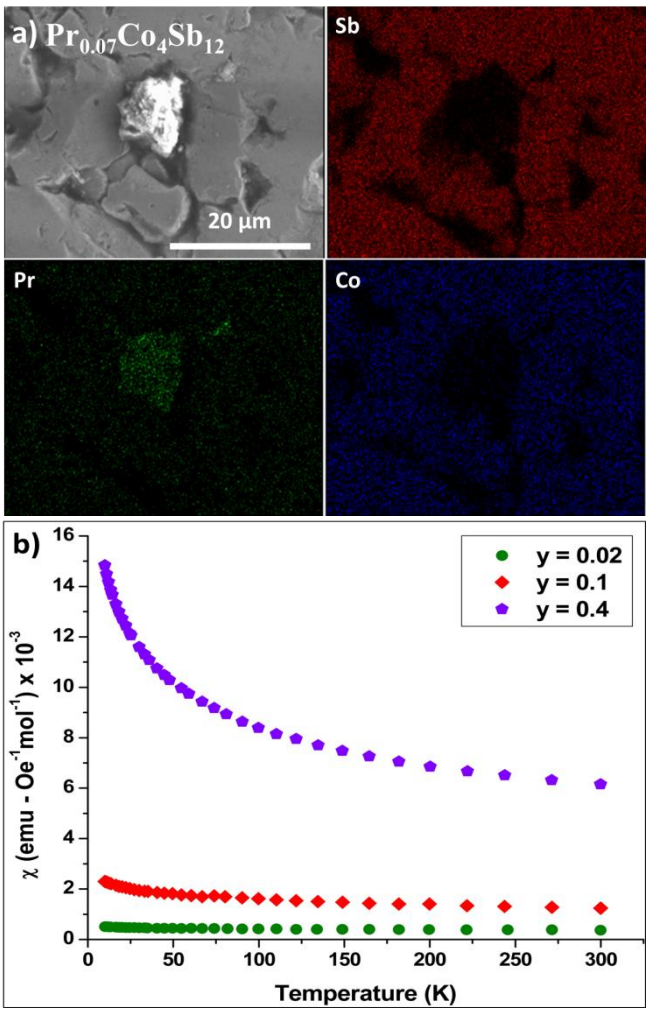

Figure 2. Energy dispersive x-ray spectroscopy (EDS) mapping of **a)** sample $Pr_{0.1}Co_4Sb_{12}$ with Sb in red, Pr in green, and Co in blue, respectively. Pr conglomerates on the grain edges (etched areas) and within the grains. Temperature dependence of **b)** molar susceptibility with increasing susceptibility over the entire temperature range as Pr is added.

Pristine Co_4Sb_{12} was prepared as a standard comparison to the Pr added Co_4Sb_{12} system, $Pr_yCo_4Sb_{12}$ ($0 < y < 0.8$). From the literature, Co_4Sb_{12} is considered a multi-band system with a very narrow direct gap of 0.25-0.3 eV at the Γ-point, which is comparable to the estimated band gap of the prepared sample via the Goldsmid-Sharp band gap estimation equation,

$$E_g = 2*e*\alpha_{max}*T_{max}$$

where e is elementary charge and α_{max} is the maximum Seebeck coefficient peaks at a characteristic temperature, T_{max} [42]. From α measurement performed on the prepared pristine sample the predicted E_g value is 0.22 eV, a value comparable to the literature. The large transition in α from ≈ 50 μVK^{-1} to ≈ 300 μVK^{-1} observed in **Figure 1(a)** also is consistent with a narrow band gap material. Former documented band structure of Co_4Sb_{12} at the Γ-point specifies that the conduction band comprises three electron-like bands (one heavy and two light) while the valence band contains one light hole-like band.[43-45] Because of the light hole-like band at the valence band edge, the Fermi level (μ_θ) of pristine

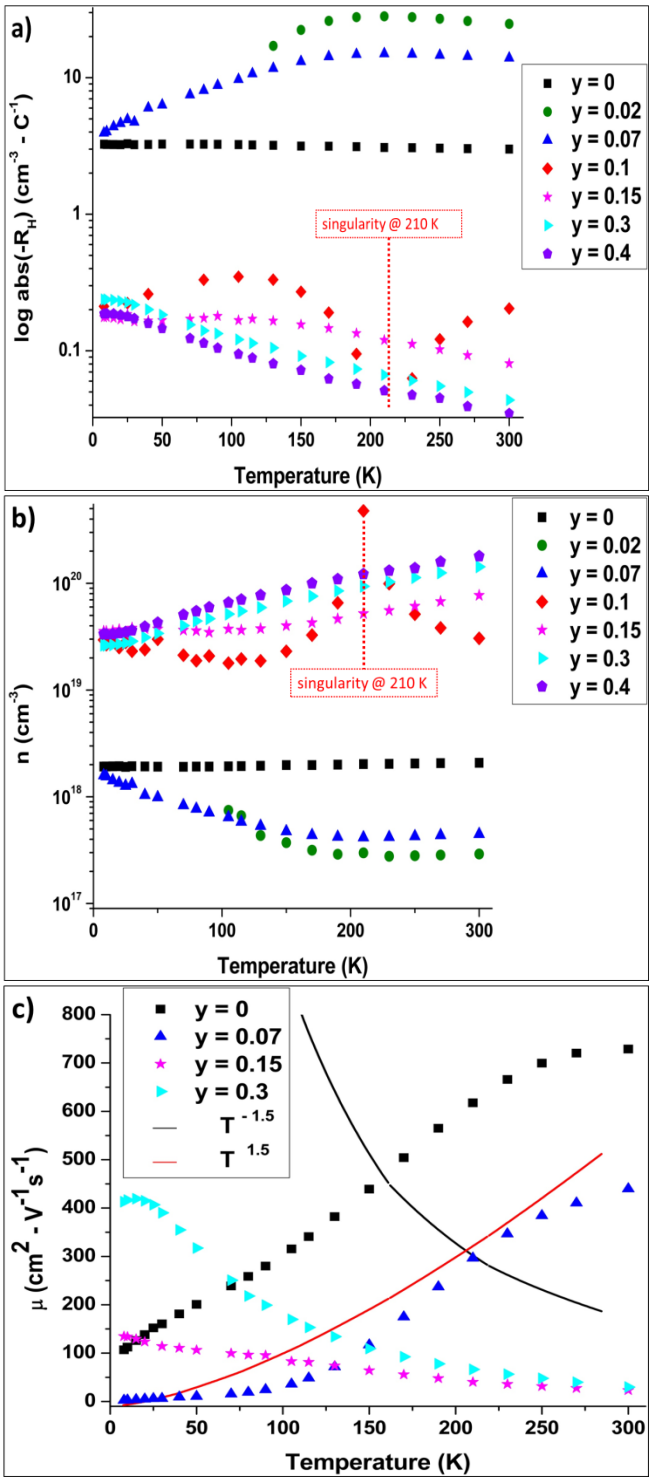

Figure 3. Temperature dependence of the TE properties of $Pr_yCo_4Sb_{12}$: **a)** Hall coefficient (R_H) with opposite sign of α indicative of the multi-band nature of the electron band structure. A singularity is seen in R_H of sample $Pr_{0.1}Co_4Sb_{12}$ and is highlighted by the dotted red line and of **b)** log carrier concentration (n) clearly presenting initial decrease in n at low concentrations of Pr ($y \leq 0.07$) and singularity in sample $y = 0.1$ at ≈ 210 K (highlighted by dotted red line), and of **c)** mobility (µ) with only 4 representative behaviors included for clarity and guide lines for comparison between characteristic phonon-electron ($T^{1.5}$) and phonon-defect coupling ($T^{-1.5}$).

Co_4Sb_{12} sits closest to this maximum[46]. Electron Microprobe Analysis (EPMA) along with *p*-type behavior (**Figure 1(a)**) seen in Co_4Sb_{12} verify that there exists a small amount of Sb excess in the pristine of $Co_4Sb_{12+0.12}$.

The as-prepared $Pr_yCo_4Sb_{12}$ ($0.02 < y < 0.4$) samples can be categorized and compared via three regimes by way of their thermoelectric behavior, in line with the nominal Pr content. **Regime I**: low concentrations of Pr ($y = 0.02$ and $y = 0.07$), **regime II**: mid concentrations of Pr ($y = 0.1$ and $y = 0.15$), and **regime III**: high concentrations of Pr ($y = 0.3$ and $y = 0.4$). As discernable in **Figure 1(a)** and **Figure 1(b)**, all samples are classified by their Pr concentration and the resulting TE behavior. For example, from **Figure 1(a)**, samples in **regime I** are *p*-type, samples in **regime II** change sign around 400 K, whereas samples in **regime III** are completely *n*-type. The following discussion will then mirror experimental evidence of these three regimes.

Regime I: Shi *et al.*[32] assert that stoichiometric $I_yCo_4Sb_{12}$, where *I* is a dopant, *always* has *n*-type conduction. However, because of the narrow band gap of Co_4Sb_{12}, it is common, depending on synthesis and experimental techniques, to observe either *p*-type or *n*-type conduction in the pristine materials.[47-51] Although the as prepared pristine Co_4Sb_{12} shows *p*-type behavior, an exotic behavior in α occurs as Pr is introduced to the matrix. At the onset of Pr addition, the dominant carriers *remain p-type and the magnitude of p-type thermopower increases*. For this work, assuming the μ_θ resides *within* the valence band, it is inferred that Pr initially begins to fill the valence band introducing more carriers and thus shifting the μ_θ closer to the conduction band (explaining the initial increase in magnitude of α, **Figure 1(a)**). Once the μ_θ reaches the critical point ($y \approx 0.07$) electrons become the dominant carriers and the samples have predominantly *n*-type conduction. Furthermore, samples below this critical Pr concentration tend to have semiconductor type σ behavior, more resistive and more temperature dependent (**Figure 1(b)**). SEM imaging elucidates the chemical role of Pr as it is added to pristine Co_4Sb_{12}. From these images and additional EDS mapping, Pr, in regime I, enters the voids (too large for substitutional doping – ionic radius of Co^{3+} is 68.5 pm and Pr^{3+} is 99 pm and Pr^{4+} is 85 pm),[52] and organizes in pockets in between grains (**Figure 2(a)**). These aggregates of poly-dispersed inclusions are expected to play a limited role in electrical and thermal transport causing electrons and phonons to bypass. A more widespread distribution of the secondary phase in between grains occurs via increase in Pr content. Knowing this, it is inferred that Pr^{4+} (non-magnetic) is filling the void spaces, whereas Pr^{3+} (magnetic) is forming the secondary phase at the grain boundaries. This argument is supported by an increase in molar susceptibility (χ) via **Figure 2(b)** (measured by a Vibrating Sample Magnetometer on a Quantum Design® PPMS system). In contrast, the Pr entering the grains behave more as charged point defects contributing to electrical transport by charge transfer and scatter phonons at elevated temperatures, which is substantiated by an increase in σ, in regime I. Additionally, Hall coefficient ($R_H = -1/ne$, where *n* is carrier concentration) measurements, (performed on a Quantum Design® PPMS system) in **Figure 3(a)**, indicate that the sign of the R_H, is negative. This means, at low concentrations of Pr, the sign of α and R_H are opposite. While the R_H involves the variation of the carriers with high mobility, the α reflects more the variation of carriers with higher effective mass. The opposite sign in α and R_H exposes the multi-band nature of the electron band structure. Overall, it is determined that the valence band is initially only partially filled for the pristine and low concentrations of Pr samples; therefore, creating a lighter hole-like band with the μ_θ closest to the valence band inhibiting *n*-type behavior until enough carriers are introduced that a saturation point is met at $y \approx 0.07$. This influence on the electron band structure is also corroborated by an initial decrease in *n* as Pr concentration increases (**Figure 3(b)**). This reduction can be understood as compensation doping.[53] More thoroughly, Pr is a donor into the Co_4Sb_{12} system, but the mass action law, $n_i^2 = np$, must be obeyed, resulting in recombination and thus initially lower *n*, which is also confirmed by a ZERO point in Hall coefficient, as seen in the singularity of **Figure 3(a)**. So, as Pr is added to Co_4Sb_{12} it fills the valence band until the material becomes fully compensated around $y > 0.07$. Using *n* (or R_H) and σ, mobility, $\mu = \sigma/ne$, can be estimated. Regarding the μ in **Figure 3(c)**, there is

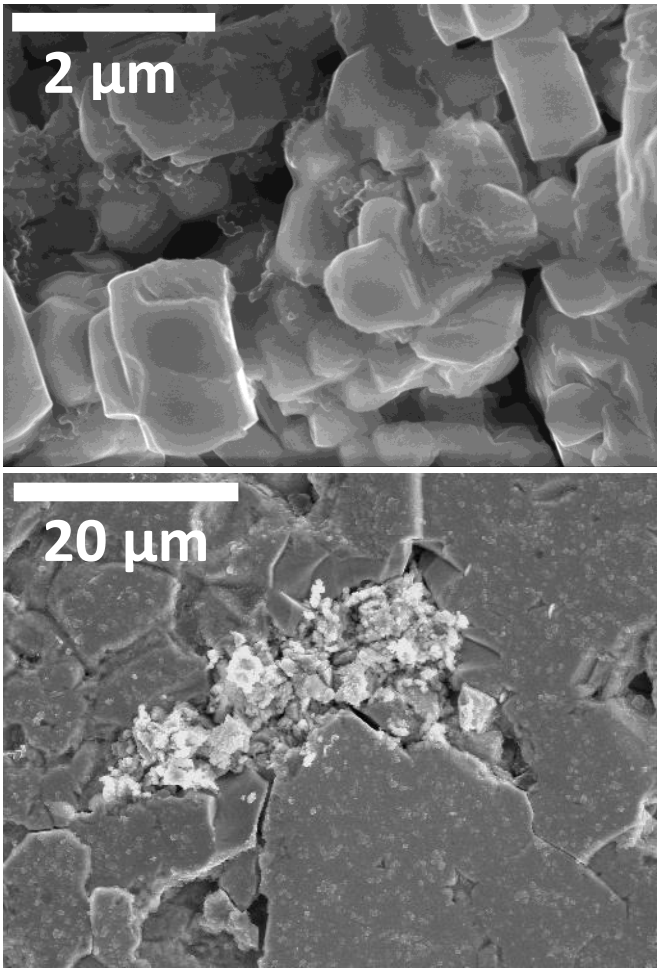

Figure 4. SEM images of a Pr nano-sized secondary phase dispersed homogeneously on the grains of a representative sample in regime III.

distinguished temperature dependence with Pr addition. At low Pr concentrations ($y \leq 0.07$) the temperature dependent μ is typical of charged point defect scattering, seen in **Figure 3(c)** as exhibiting a $T^{1.5}$ behavior, which is congruent with the idea that Pr fills the cages

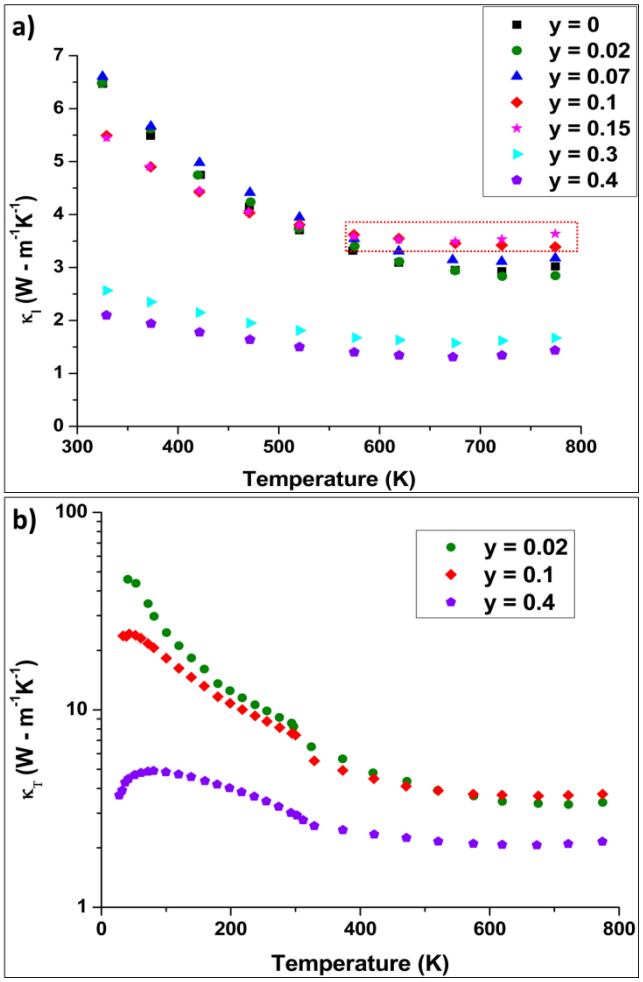

Figure 5. Temperature dependence of the TE properties of $Pr_yCo_4Sb_{12}$: **a)** lattice thermal conductivity (κ_l) showing phonon-phonon scattering as the primary scattering mechanism at high temperatures, with bipolar conduction highlighted in regime II by the red dotted line, and of **b)** showing full temperature range (10 K – 750 K) of total thermal conductivity (κ_T), with radiation correction highlighting the drop in magnitude of κ_T at low temperatures.

first, has charge transfer, and as a result becomes an ion in the void space.

Regime II and III: The turnover in α in regime II further confirms that at higher temperatures intrinsic or minority type conduction dominates, again consistent with multi-band behavior and effect of dual carrier types on the band structure as described above. Since acceptors are the dominant carrier type in the pristine material, Pr acts as a counter dopant to *p*-type Co_4Sb_{12} causing an eventual turnover to *n*-type (**Figure 1(a)**). The multi-band nature also alludes to band structure manipulation with the μ_θ shifting closer to the conduction band as Pr is added to the pristine by the presence of the turnover from *p*-type to *n*-type in α. As the filling fraction of Pr is increased in regime II and III, α_{max} also shifts to higher temperatures (**Figure 1(a)** ≈ 200 K) due to deviations in band structure and the onset of minority carrier contributions. This progressive trend of the α peak is significant because it up-shifts the peak in ZT and thus favors higher temperature power generation applications. A slight reduction in α is observed (from 10 K to 550 K) as the amount of Pr is increased into the system from y = 0.1 to y = 0.4, as expected for heavily doped *n*-type semiconductors. This trend is verified by a rise in *n* (**Figure 3(b)**). At the point where TE behavior begins to dramatically change, close to y ≈ 0.07, a transformation also occurs in *n* by way of an increase of two orders of magnitude. The fully compensated nature of regime II also arises from the multi-band environment of the system. Temperature dependent μ, in regime III, follows $T^{-1.5}$ behavior consistent with electron-phonon coupling, while regime II appears to be somewhere in between the behavior depicted in regime I and III (**Figure 3(c)**). The detailed forms of mobility constitute convincing evidence that conduction electrons are primarily scattered by secondary phase interactions at low temperatures. In all regimes, Pr enters the empty cages and agglomerates in between the grains; however, SEM and EDS confirm a nano-sized Pr secondary phase on the grain boundaries in regime II and III, seen in **Figure 4**. The presence of this nano-sized Pr secondary phase is dramatically enlarged from regime II to regime III. In **Figure 1(b)**, Kondo-like behavior is observed in regime III at low temperatures, further signifying that Pr^{4+} ions are filling the voids and Pr^{3+} ions are forming the secondary phase. In regime III, Pr contributes the most electrons; hence a higher σ (**Figure 1(b)**). Samples in regime III exhibit a degenerate semiconductor type behavior, more conducting and relatively less temperature dependent, while samples in regime II have behaviors that lie between regime I and III. This degenerate type behavior in regime III, specifically at very low temperatures, suggests samples are fully filled; hence, having fewer vacancies to scatter electrons with a profound effect on lattice thermal conductivity (κ_l) from the new homogeneous nano-phase contributions located on the grain boundaries. κ_l is calculated by the equation $\kappa_l = \kappa_T - \kappa_c$, where κ_c is the carrier thermal conductivity, given by the Wiedemann–Franz relation $\kappa_c = L_0\sigma T$, where the Lorenz constant is $L_0 = 2 \times 10^{-8}\ V^2\ K^{-2}$, a value typically used for heavily doped semiconductors, and κ_T is total thermal conductivity. At high temperatures, regime I and II have analogous κ_l suggesting a comparable concentration of short range imperfection due to Pr point defects; conversely, regime III has a much lower κ_l at both high and low temperatures strongly suggesting Pr point defect concentration is much higher in this regime (**Figure 5(a)**). The dominant heat carrying phonon wavelength (λ_{ph}) can be estimated by a rule of thumb,

$$\lambda_{ph} = a*(T_\theta/T)^{[54]}$$

where a is lattice constant of the material, T_θ is Debye temperature, and T is temperature. Applying this approximation to the Pr added Co_4Sb_{12} samples it is apparent at low temperatures (< 100 K) that λ_{ph} values are on the order of 10 nm, which is orders of magnitude smaller than the average grain of the primary phase (≈ 10-20 μm). Therefore, the decline of κ_l correspondingly with the increase in Pr, at low temperatures (**Figure 5(a)**), *cannot* be solely contributed to grain boundary scattering. The drop must be marked as phonon point defect scattering and/or scattering of the nano-sized secondary phase on the grain boundary. Because of the multi-band collaboration of this narrow band gap degenerate semiconductor, κ_c can no longer be considered the sum of the partial conductivities from each type of carrier, holes and electrons. According to Nolas,[55] there is a third term, the bipolar term, which results from Peltier heat flow allowable with more than one type of carrier. In regime II there is a noticeable upturn in κ_l for temperatures > 550 K (**Figure 5(b)**), which is attributed to bipolar conduction. This is verified by the same upturn seen in α (**Figure 1(a)**) of regime II. **Figure 5(b)** definitively confirms the κ_l component of κ_T dominates for all samples, suggesting phonon-phonon scattering as the primary scattering mechanism at high temperatures. The κ_T reduction between regime I,

II and regime III occurs via phonon scattering from the presence of the poly-dispersed secondary phase located on the grain boundaries.

Conclusions

From pristine Co_4Sb_{12} to $Pr_{0.3}Co_4Sb_{12}$, σ increases by a factor of 3. Due to the increase in σ, the overall power factor ($PF = \alpha^2\sigma T$) increases from 0.1 W-m^{-1}K^{-1} for Co_4Sb_{12} to 2.5 W-m^{-1}K^{-1} for $Pr_{0.3}Co_4Sb_{12}$ (**Figure 6(a)**). As a result of the PF enhancement, and the drop in κ_T, as the filling fraction of Pr is increased, an increase in the maximum ZT for samples $Pr_yCo_4Sb_{12}$ ($0.2 < x < 0.4$) is noted with a $ZT_{max} \approx 1.0$ at 775 K (**Figure 6(b)**). A turnover in ZT occurs at higher temperatures (≈ 150 K shift) as Pr is added due to population of the bands and the onset of the bipolar effect as observed in the Seebeck coefficient and in the lattice thermal conductivity. Samples above y = 0.4, $Pr_yCo_4Sb_{12}$ ($0.5 < y < 0.8$), were difficult to synthesize and showed reduction in TE efficiency with a decrease in electrical transport properties, giving rise to a possible limit to improvement of TE properties, and thus ZT, of this material at $y \approx 0.4$. The results reported herein are the first experimental investigation of the TE properties of a series of single-filled Praseodymium Co_4Sb_{12}-based skutterudite samples. Exotic behavior in thermopower occurred for samples $y < 0.15$, including *p*-type behavior seen in regime I and minority carrier dominance at high temperatures in regime II. The suggested approach of *surpassing the FFL* of single-filled $Pr_yCo_4Sb_{12}$ for improving TE properties was experimentally successful. Pr effectively acted as *one control parameter*, not only improving the PF of reported samples from PF ≈ 0.1 W m^{-1} K^{-1} to PF ≈ 2.5 W m^{-1} K^{-1} at 775 K, but also reducing κ_T from $\kappa_T \approx 4.5$ W m^{-1} K^{-1} to $\kappa_T \approx 2.5$ W m^{-1} K^{-1} at 775 K, leading to an 21-fold increase in ZT, from ZT ≈ 0.05 at 675 K for the pristine to ZT ≈ 1.0 at 775 K for $Pr_{0.4}Co_4Sb_{12}$. This enhancement indicates that the TE properties can indeed be improved by purposefully exceeding the FFL of single-filled $Pr_yCo_4Sb_{12}$. This approach may also be useful and has the potential of being investigated in other single-filled Co_4Sb_{12}-based skutterudites and clathrates.

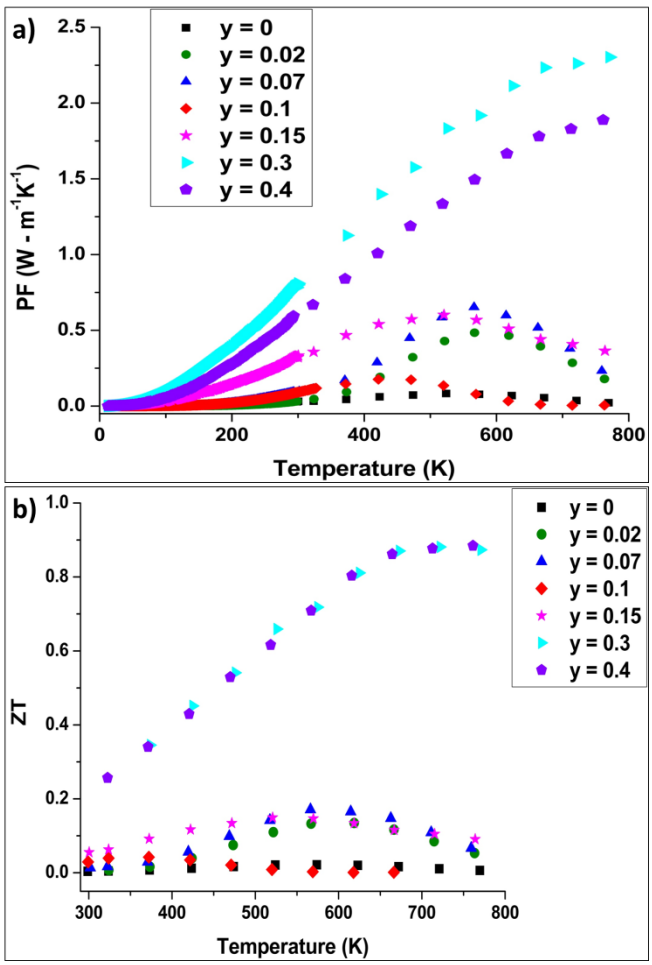

Figure 6. Temperature dependence of the TE properties of $Pr_yCo_4Sb_{12}$: **a)** Power Factor (PF) showing an overall increase in the electrical properties as Pr is added, and of **b)** Figure of Merit (ZT) showing an overall increase in ZT as Pr is added above FFL.

Acknowledgements

This work was supported by a DOE/EPSCoR Implementation Grant (#DE-FG02-04ER-46139), and the SC EPSCoR cost-sharing program. We'd also like to thank Dr. L.A. Dempere with the Major Analytical Instrumentation Center (MAIC) and Particle Analysis Instrumentation Center (PAIC) at the University of Florida in Gainesville, FL 32611, USA for EPMA and microscropy analysis.

Notes and References

[*] Prof. T. M. Tritt, Department of Physics and Astronomy, Clemson University Clemson, SC 29634, USA E-mail: jwhubba@g.clemson.edu, ttritt@clemson.edu

†Supplementary information can be found in the supplementary material section.

_[1] W.J. Xie, J. He, S. Zhu, X.L. Su, S.Y. Wang, T. Holgate, J.W. Graff, V. Ponnambalam, S.J. Poon, X.F. Tang, *Acta Mater.* **2010**, 58, 14.
_[2] B. C. Sales, D. G. Mandrus, B. C. Chakoumakos in *Semiconductors and Semimetals*, Vol. 70 (Eds: T. M. Tritt), Academic Press, Waltham, United States of America, 2001, Ch. 1.
_[3] M. Christensen, F. Juranyi, B. B. Iversen, *Physica B: Cond. Matter* 2006, 385-386, 1.
_[4] Y. Takasu, T. Hasegawa, N. Ogita, M. Udagawa, M. A. Avila, K. Suekuni, T. Takabatake, *PRL* **2008**, 100**,** 165503.
_[5] I. K. Dimitrov, M. E. Manley, S. M. Shapiro, J. Yang, W. Zhang, L. D. Chen, Q. Jie, G. Ehlers, A. Podlesnyak, J. Camacho, Q. Li, *Phys. Rev. B.* **2010**, 82, 174301.
_[6] V. Keppens, D. Mandrus, B. C. Sales, B. C. Chakoumakos, P. Dai, R. Coldea, M. B. Maple, D. A. Gajewski, E. J. Freeman, S. Bennington, *Nature* **1998**, 395, 876-878.
_[7] X. Gao, M. S. Daw, *J. Phys.: Condens. Matter* **2009**, 21, 045401.
_[8] G. P. Meisner, D. T. Morelli, S. Hu, J. Yang, C. Uher, *PRL* **1998**, 80, 16.
_[9] G. S. Nolas, M. Kaeser, R. T. Littleton IV, T. M. Tritt, *Appl. Phys. Lett.* **2000**, 77, 12.
_[10] B. C. Sales, B. C. Chakoumakos, D. Mandrus, *Phys. Rev. B* **1999**, 61, 4.
_[11] X. Y. Zhoa, X. Shi, L. D. Chen, W. Q. Zhang, W. B. Zhang, *J. Appl. Phys.* **2006**, 99 053711.
_[12] V. L. Kuznetsov, L. A. Kuznetsova, D. M. Rowe, *J. Phys.: Condens. Matter* 2003, 15 5035-5048.
_[13] G. S. Nolas, J. L. Cohn, G. A. Slack, *Phys. Rev. B* **1998**, 58, 1.

_[14] T. He, J. Chen, H. D. Rosenfeld, M. A. Subramanian, Chem. Mater. **2008**, 18, 759-762.
_[15] D. T. Morelli, G. P. Meisner, B. Chen, S. Hu, C. Uher, *Phys. Rev. B.* **1997**, 56 12.
_[16] L. D. Chen, T. Kawahara, X. F. Tang, T. Goto, T. Hirai, J. S. Dyck, W. Chen, C. Uher, *J. Appl. Phys.* **2001**, 90, 4.
_[17] S. Q. Bai, Y. Z. Pei, L. D. Chen, W. Q. Zhang, , X. Y. Zhao, J. Yang, *Acta Mater.* **2009** 3135-3139.
_[18] H. Li, X. Tang, Q. Zhang, C. Uher, *Appl. Phys. Lett.* **2009**, 94, 102114.
_[19] J. Y. Peng, P. N. Alboni, J. He, B. Zhang, Z. Su, T. Holgate, N. Gothard, T. M. Tritt, *J. Appl. Phys.* **2008**, 104, 053710.
_[20] J. R. Salvador, J. Yang, H. Wang, X. Shi, *J. Appl. Phys.* **2010**, 107, 1.
_[21] X. Shi, H. Kong, C.-P. Li, C. Uher, J. Yang, J. R. Salvador, H. Wang, L. D. Chen, W. Zhang, *Appl. Phys. Lett.* **2008**, 92, 182101.
_[22] Xi L., J. Yang, W. Zhang, L. D. Chen, J. Yang, *J. Am. Chem. Soc.* **2009**, 191, 5560-5563.
Mallik R., Stiewe C., Karpinski G., Hassdorf R., Muller E., *J. Electron. Mater.* **38** 7 (2009).
_[23] S. Ballikaya, N. Uzar, S. Yildirim, J. R. Salvador, C. Uher, *J. Solid State Chem.* **2012**, 193, 31-35.
_[24] J. K. Lee, S. M. Choi, W. S. Seo, Y. S. Lim, H. L. Lee, I. H. Kim, *Renewable Energy* **2012**, 42, 36-40.
_[25] L. Zhang, A. Grytsiv, P. Rogl, E. Bauer, M. Zehetbauer, *J. Phys. D: Appl. Phys.* **2009** 42 225405.
_[26] X. Shi, J. Yang, J. R. Salvador, M. Chi, J. Y. Cho, H. Wang, S. Bai, J. Yang, W. Zhang, L. D. Chen, *J. Am. Chem. Soc.* **2011**, 133, 7837-7846.
_[27] J. W. Graff, S. Zhu, T. Holgate, J. Y. Peng, J. He, T. M. Tritt, *J. Electron. Mater.* **2011**, 40, 5.
_[28] M. Christensen, A. B. Abrahamsen, N. B. Christensen, F., Juranyi, N. H. Andersen, K. Lefmann, J. Andreasson, C. R. H. Bahl, B. B. Iverson, **2008** *Nature Mater.* 7, 811 – 815.
_[29] M. M. Koza, M. R. Johnson, R. Viennois, H. Mutka, L. Girard, D. Ravot, *Nature Mater.* **2008**, 7, 805-810.
_[30] X. Shi, W. Zhang, L. D. Chen, J. Yang, *PRL* **2005**, 95 185503.
_[31] Y. Pei, H. Wang, G. J. Snyder, *Adv. Mater.* **2012**, 24, 6125-6135.
_[32] X. Shi, S. Bai, L. Xi, J. Yang, W. Zhang, L. D. Chen, *J. Mater. Res.* **2011** 26 15.
_[33] K. Abe, H. Sato, T. D. Matsuda, T. Namiki, H. Sugawara, Y. Aoki, *J. Phys.: Condens. Matter* **2002** 14, 11757.
_[34] E. D. Bauer, N. A. Frederick., P. –C. Ho, V. S. Zapf, M. B. Maple, *Phys. Rev. B* **2002**, 65, 100506.
_[35] H. Sato, H. Sugawara, D. Kikuchi, S. Sanada, K. Tanaka, H. Aoki, K. Kuwahara, Y. Aoki, M. Kohgi, *Physica B* **2006**, 378-380, 46-50.
_[36] C. Sekine, T. Uchiumi, I. Shirotani, T. Yagi, *Phys. Rev. Letters* **1997** 79, 17.
_[37] K. Tanaka, D. Kikuchi, Y. Kawahito, M. Ueda, H. Aoki, K. Kuwahara, H. Sugawara, Y. Aoki, H. Sato, *Physica B* **2008**, 866-868.
_[38] O. Tougait, D. Kaczorowski, H. Noel, *J. Solid State Chem.* **2005**, 178, 3639-3647.
_[39] M. S. Toprak, C. Stiewe, D. Platzek, S. Williams, L. Bertini, E. Muller, C. Gatti, Y. Zhang, M. Rowe, M. Muhammed, *Adv. Func. Mater.* **2004**, 14, 12.
_[40] A.L. Pope, B. Zawilski, and T.M. Tritt, *Cryogenics* **2001**, 41, 725.
_[41] A. L. Pope, R. T. Littleton, IV, T. M. Tritt, *Rev. Sci. Instrum.* **2001** 72 3129.
_[42] H. J. Goldsmid, J. W. Sharp, *J. Electron. Mater.* **1999**, 28, 7.
_[43] D. J. Singh, W. E. Pickett, *Phys. Rev. B* **1994**, 50, 15.
_[44] L. Hammerschmidt, S. Schlecht, B. Paulus, *Phys. Status Solidi A* **2013**, 210, 1.
_[45] Y. Zhu, H. Shen, L. Zuo, H. Guan, *Solid State Communications* **2011**, 151, 1388-1393.
_[46] C. Kittel in Introduction to Solid State Physics, 8th Ed., John Wiley and Sons, Inc., Hoboken, United States of America, 2004, ch. 7
_[47] J. P. Fleurial, T. Caillat, A. Borshchevsky, *Proceedings of the XVI International Conference on Thermoelectrics*, Dresden, Germany, **1997**.
_[48] J. Ackermann, A Wold, *J. Phys. Chem. Solids* **1977**, 38, 1013-1016.